A theranostic approach based on the use of a dual *boron*/Gd agent to improve the efficacy of Boron Neutron Capture Therapy in the lung cancer treatment

Diego Alberti, PhD[a], Nicoletta Protti, PhD[b,c], Antonio Toppino, PhD[d], Annamaria Deagostino, PhD[d], Stefania Lanzardo, PhD[a], Silva Bortolussi, PhD[b,c], Saverio Altieri, PhD[b,c], Claudia Voena, PhD[a,e], Roberto Chiarle, MD[a,e,f], Simonetta Geninatti Crich, PhD[a,*], Silvio Aime, PhD[a]

[a]*Department of Molecular Biotechnology and Health Sciences; University of Torino, Torino, Italy*
[b]*Department of Nuclear and Theoretical Physics, University of Pavia, Pavia, Italy*
[c]*Nuclear Physics National Institute (INFN), section of Pavia, Pavia, Italy*
[d]*Department of Chemistry, University of Torino, Torino, Italy*
[e]*Center for Experimental Research and Medical Studies (CERMS), Città della Salute e della Scienza, Torino, Italy*
[f]*Department of Pathology, Children's Hospital Harvard Medical School, Boston, MA, USA*

Received 3 August 2014; accepted 8 December 2014

Abstract

This study aims at developing an innovative theranostic approach for lung tumor and metastases treatment, based on Boron Neutron Capture Therapy (BNCT). It relies on to the use of low density lipoproteins (LDL) as carriers able to maximize the selective uptake of boron atoms in tumor cells and, at the same time, to quantify the in vivo boron distribution by magnetic resonance imaging (MRI). Tumor cells uptake was initially assessed by ICP-MS and MRI on four types of tumor (TUBO, B16-F10, MCF-7, A549) and one healthy (N-MUG) cell lines. Lung metastases were generated by intravenous injection of a Her2+ breast cancer cell line (i.e. TUBO) in BALB/c mice and transgenic EML4-ALK mice were used as primary tumor model. After neutron irradiation, tumor growth was followed for 30-40 days by MRI. Tumor masses of boron treated mice increased markedly slowly than the control group.

From the Clinical Editor: In this article, the authors described an improvement to existing boron neutron capture therapy. The dual MRI/BNCT agent, carried by LDLs, was able to maximize the selective uptake of boron in tumor cells, and, at the same time, quantify boron distribution in tumor and in other tissues using MRI. Subsequent in vitro and in vivo experiments showed tumor cell killing after neutron irradiation.

Key words: Low density lipoproteins (LDL); Boron Neutron Capture Therapy (BNCT); MRI; Theranostic agents; Carboranes

Background

Lung cancer remains the leading cause of cancer-related mortality (www.who.int/cancer/en) causing 1.59 million death worldwide per year. Lungs are the most common sites of metastatic disease and tumor relapse after the treatment of the primary mass. Since lung tumors are largely disseminated in the pulmonary parenchyma, their excision is often difficult and not resolving causing a median survival time of less than 1 year. For these reasons it is important to develop less invasive treatments able to discriminate between healthy and pathological tissues at cellular level. Boron neutron capture therapy (BNCT) is an experimental binary radiation therapy currently under intense scrutiny for the treatment of cancer, especially head and neck recurrent tumors,[1] skin melanomas,[2] liver metastatic diseases[3] and brain tumors.[4] It is based on thermal neutron capture by ^{10}B

This research was founded by the AIRC Investigator Grant IG2013, by the University of Torino (project code D15E11001710003), by the University of Genova (Progetto San Paolo; Title: Validazione di molecole per il rilascio tumore specifico di farmaci e la valutazione contestuale della risposta mediante imaging funzionale), by MIUR (PRIN 2012 code 2012SK7ASN) and by Consorzio Interuniversitario di Ricerca in Chimica dei Metalli dei Sistemi Biologici (CIRCMSB). This research was performed in the framework of the EU COST Action TD1004.

The authors declare no conflict of interest.

Part of this work was presented at the joint annual meeting of ISMRM-ESMRMB held in Milano (Italy) 10-16 May 2014 and at the European Molecular Imaging Meeting (EMIM) held in Torino (Italy) 26-28 May 2013.

*Corresponding author at: Department of Molecular Biotechnology and Health Sciences, University of Torino, via Nizza 52, Torino, Italy.

nuclei previously delivered to tumor cells. The neutron capture event results in the formation of excited ^{11}B that decay emitting highly ionizing $^{4}He^{2+}$ and $^{7}Li^{3+}$ ions. Cell death is triggered by the release of the energy of these charged particles which create ionization tracks along their trajectories in a range of approximately 5–9 μm. Thus it is possible to destroy tumor cells without affecting adjacent healthy cells if ^{10}B atoms are selectively accumulated in the intracellular space. It has been estimated that approximately 10-30 μg of *boron* per gram of tumor mass is needed to attain an acceptable therapeutic advantage, provided the availability of a suitable neutron source and considering an acceptable irradiation time.[5,6] This fact makes BNCT a promising option for the treatment of disseminated tumors, such as pulmonary metastases that cannot be treated by methods requiring a precise localization of the pathological tissue, like surgery, conventional photon-therapies or heavy ion-therapy. The selective delivery to tumor cells is crucial to increase the amount of internalized boron maintaining, at the same time, a low concentration in surrounding healthy tissues and in blood to minimize damage. Currently, two BNCT drugs are available for clinical investigation namely: i) L-para-boronophenylalanine (BPA), structurally related to the amino acid phenylalanine, that has been used in clinical trials to treat glioblastoma, head and neck recurrent cancer and melanoma[7] and ii) sodium mercaptoundecahydro-closo-dodecaborate (BSH) that has been investigated for the treatment of malignant glioma.[8] Despite their clinical use, both BPA and BSH show low selectivity and great efforts have been made by several research groups to develop new and more selective *boron* delivery agents. To this purpose, polynuclear boron derivatives, especially carboranes, have been extensively investigated.[9] Carboranes are icosahedral cages containing 10 *boron* atoms and they have been used to design boron delivery vehicles due to their high *boron* content, chemical versatility and in vivo stability.[10,11] Carborane based agents may be functionalized with small targeting moieties including amino acids, vitamins, carbohydrates, porphyrinates, ect[12] to achieve tumor selectivity. A different strategic concept for selectively introducing *boron* into tumor cells is based on the covalent binding of multiple carborane cages to monoclonal antibodies[13] or their incorporation into large entities such as, liposomes,[14,15] low-density lipoproteins[16-18] (LDL) or other nanoparticles. Despite the current availability of many carborane derivatives that have given significant results in preclinical studies, none has been translated to the clinical setting. A crucial issue to reach this goal is the assessment of the *boron* amount in the tumor tissue. This is important in order to proceed with the neutron irradiation, because successful results can only be expected if the boron concentration threshold has been reached, and if a proper dose prescription is performed according to the therapeutic goal and the sparing of the normal tissue. Currently, *boron* concentrations in tumor are estimated in clinical trials using empirical data models that depend on tumor-to-blood, tumor-to-brain and brain-to-blood boron concentration ratios. One of the problems is that the uptake and distribution of boron varies among patients and that large uncertainties exist in the tumor-to-blood boron concentration ratio.[19] Only proper neutron capture therapy (NCT) agent design, based on an improved knowledge of how molecules enter healthy and cancer cells, could allow the optimal intracellular concentration, needed to make NCT an effective therapy to cure cancer, to be reached. Furthermore, the access to not invasive and highly sensitive imaging techniques can allow the detection of tumor *boron* concentration in real time before neutron treatment. Some of these methodologies require the functionalization of the NCT agent with a proper imaging reporter, such as ^{18}F atoms for Positron Emission Tomography (PET), a Gd/Fe containing agent for Magnetic Resonance Imaging (MRI) or ^{19}F atoms for ^{19}F-NMR. Both PET and MRI detection limits are below the boron threshold necessary to perform the therapy.[20] PET is more sensitive but it has the disadvantage of the administration of further radioactivity, while MRI appears to be a suitable technique to achieve the goal of the quantitative assessment of the NCT agent in tissues. Although its sensitivity is lower in comparison to nuclear and optical modalities, the high spatial resolution (<100 μm) of MRI provides detailed morphological and functional information, and the absence of ionizing radiation makes it safer than techniques based on the use of radioisotopes. MRI signal is dependent on the longitudinal (T_1) and transverse (T_2) proton relaxation times of water and in both clinical and experimental settings the endogenous contrast can be altered by the use of contrast agents (CA) that decrease T_1 and T_2 of water protons in the tissues where they distribute.[21] In a proton MR image there is a direct proportionality between the observed signal intensity (SI) enhancement and the concentration of the CA. Thus these agents can be used to carry out indirect *boron* quantification upon their linking to the neutron capture compound. Interestingly, a given cell can be visualized by MRI when the number of Gd^{3+} complexes is of the order of 10^{8}-10^{9} per cell, i.e. a threshold close to the number of *boron* atoms necessary to provide an effective NCT treatment.[22]

This study is aimed at testing the efficiency of an MRI theranostic agent for BNCT treatment of lung tumors and metastases. Lung metastases have been generated by intravenous injection of a $Her2^{+}$ breast cancer cell line (TUBO).[23] The Her2 overexpression has been detected in approximately 20% of human breast cancers and is associated with an aggressive course and with early development of metastases. Several anti-Her2 strategies has been approved revolutionizing the clinical outcome of $Her2^{+}$ breast cancer, but in most cases, the succeeding onset of pharmacological resistance renders this treatments completely ineffective. In this context, the set-up of new strategies is urgently needed. As a model of primary tumor in the lung, we used a transgenic (Tg) mouse line model that ectopically expresses the oncogenic EML4-ALK fusion protein under a lung-specific SP-C promoter[24] specifically in lung alveolar epithelial cells. In all Tg mice, the EML4-ALK protein was expressed specifically in lung epithelial cells. All of the EML4-ALK transgenic mice developed many adenocarcinoma nodules in both lungs with a 100% penetrance within a few weeks after birth, as a consequence of the potent oncogenic activity of the fusion kinase EML4-ALK. The dual MRI/BNCT agent used in this study is able to maximize the selective uptake of *boron* in tumor cells by targeting LDL receptors (LDLRs), and, at the same time, to quantify *boron* distribution in tumor and in other tissues by MRI.[17] LDLs have been identified as good

carriers of *boron* cluster since the expression of LDLRs is up-regulated in many tumors.[25,26] Furthermore these nanoparticles can carry a high number of boron atoms without losing the specific internalization pathway. For NCT treatment, the AT101 ligand was chelated using $GdCl_3$ enriched in the isotope 157 to exploit its high thermal neutron cross-sections of around 255000 barns.[27] This cross-section provides a roughly 65-fold improvement upon the one of ^{10}B neutron capture. The nuclear reaction of ^{157}Gd generates prompt γ-rays of broad energy spectrum in competition with Auger electrons and X-rays. Due to their very short ranges (less than 0.5 nm up to 1.4 μm), ^{157}Gd atoms would have to be localized at the nuclei of target cells, in contact with DNA, in order to induce sufficient damage to cause apoptosis and to obtain an effective treatment.

Methods

The ^{10}B enriched ligand-*C*-[*N*-(DOTAMA-C_6)-carbamoylmethyl]C′-palmitamidomethyl-*o*-carborane (^{10}B enriched AT101) was synthesized following the previously reported procedure[17] described in Supplementary Material.

Cell and animal irradiation were performed in the thermal column of the TRIGA Mark II reactor at University of Pavia (Italy). The experimental protocol is described in the supplementary materials. The irradiation facility was previously designed for TAOrMINA treatment.[28] TRIGA maximum power is 250 kW and has a cross section of 40 × 20 cm^2, a length of 1 m and it starts at about 1.3 m from the centre of the reactor core. The irradiation time has been fixed at 15 minutes at a reactor power of 30 kW, corresponding to a thermal neutron fluence of $1.26 \cdot 10^{12}$ cm^{-2} Animal studies were performed according to the national regulations and were approved by the local ethical committee. The preparation of the animal model is described in the Supplementary Materials. *Boron* concentration in tumor, tissues and organs was calculated using the equations[29] reported in Supplementary Material.

Mice models were prepared by injecting 50000 TUBO cells into the tail vein three weeks before the treatment. The first mice group (n = 15) received AT101/LDL (0.1 mmol/kg Gd dose) 6 hours before irradiation. Group two (irradiated control group, n = 15) received at the same time, the same volume of PBS. A third group of non-irradiated mice (n = 10) was used as a reference to assess tumor growth in the absence of any treatment. The neutron field of the TRIGA Mark II is not collimated and this implies that during the lung irradiation, the whole body of the animal is indirectly exposed to the neutron field. In order to protect the healthy organs of the animal body a shield made of 95% ^6Li-enriched Li_2CO_3 powder was used as neutron absorber, due to the absence of secondary gamma radiation after ^6Li neutron capture.[30]

The simulation code Monte Carlo N-Particles (MCNP) was used to design the treatment plan. The simulation was validated with neutron flux measurements by the activation of Cu wires using the Westcott formalism.[31] In the adopted experimental set-up 5 mice are irradiated at the same time, each one protected by two units of Li_2CO_3 neutron shield to cover the head and the abdomen regions. The units are kept separated of about 1 cm to guarantee the direct exposure of the tumors to the neutron flux.

Results

LDL adduct preparation and characterization

The dual *boron*/Gd agent (AT101) used in this work (Figure 1, *A*) and its LDL adducts have been prepared following the already published procedures.[17] Briefly, since AT101 forms stable, large sized micelles in aqueous solution, it was necessary to de-assemble them by adding β-cyclodextrin (β-CD) before the incubation with LDL to yield the molecular dispersion of the amphiphilic complexes. The experimental work up consists of the step-wise addition of aliquots of the β-CD/AT101 adduct to the aqueous solution of LDL particles in order to transfer AT101 complexes to LDLs (Figure 1, *B*). The thermodynamic association constant (Ka) of AT101/LDL adducts was of 1.7×10^4 M^{-1} with an estimated number of 300 binding sites available to AT101 per protein.[17] The r_{1p} (the observed relaxation rate of a water solution containing 1 mM of a paramagnetic species) of the AT101/LDL adduct was 15.5 mM^{-1} s^{-1} and the dynamic light scattering (DLS) measurements indicated that their size was almost the same (24 ± 2 nm) as that found on the native LDL particles (23 ± 1 nm).

"In vitro" cellular uptake experiments and MRI analysis

Using the above reported method, an AT101/LDL adduct containing ca. 230 Gd complexes per protein was prepared. TUBO is a $Her2^+$ established cell line derived from a spontaneous mammary tumor arising in a virgin transgenic BALB-*neu*T female mouse. In these mice, the mammary carcinogenesis displays a histopathological course that closely recapitulates the one observed in human breast tumors,[32] making this mouse model, and the TUBO cells derived from it, an ideal tool to test anti-cancer therapies. As already reported, many tumor cells are characterized by an up-regulation of LDL transporters.[33] In order to evaluate the uptake capacity of LDLRs, TUBO cells have been incubated in the presence of increasing amounts of the AT101/LDL theranostic agent for 16 hours at 37 °C. After washing with cold PBS, cells have been collected and analyzed by ICP-MS to measure the Gd content. In order to consider the different number of cells present in each sample, the amount of Gd was normalized to the total protein concentration. The results obtained with TUBO cells (Figure 2, *A*) have been compared with those obtained with murine melanoma (B16-F10), human breast cancer (MCF-7), human lung adenocarcinoma (A549) and with healthy mouse mammary gland cells (N-MUG) using the same incubation protocol. Figure 2, *A* shows that the internalization of AT101/LDL by tumor cells (TUBO, B16-F10, MCF-7, A549) is significantly more efficient in the range of the concentrations considered than that observed with healthy N-MUG cells. Cell viability after AT101/LDL incubation have been assessed by MTT test (Figure S1 Supplementary Materials). An LDL concentration of 25 μg/mL in the culture medium was enough to internalize into the target cells a sufficient amount of *boron* to perform BNCT. In fact a Gd concentration of 1.7×10^{-9} moles/mg corresponds to

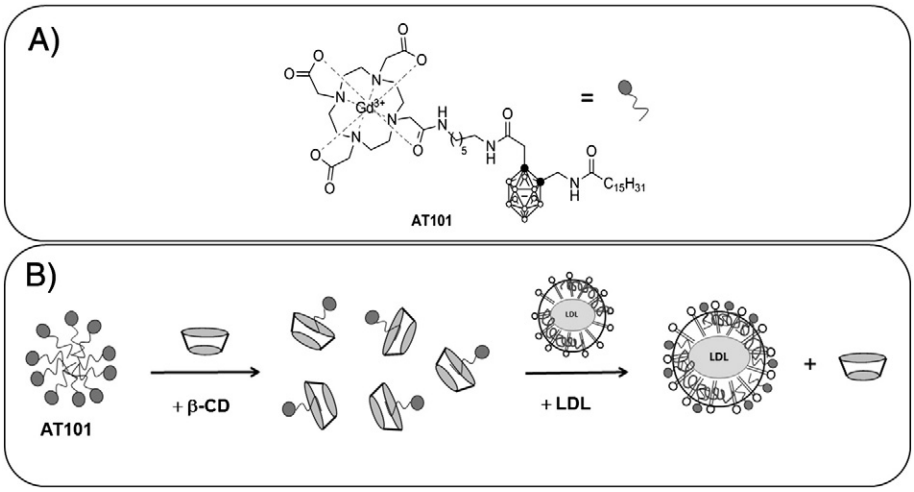

Figure 1. **(A)** Schematic representation of the dual *boron*/Gd agent (AT101). **(B)** Schematic depiction of the formation of AT101/β-CD and AT101/LDL adducts.

an intracellular *boron* concentration of 28 ppm (by considering that 1 g of tissue contains 1×10^9 cells and that 1 mg of proteins correspond to 6×10^6 TUBO cells). This concentration is sufficient to attain a successful treatment if the *boron* concentration in the surrounding tissue is at least three times lower and if a sufficient neutron fluence can be delivered to patients in an acceptable irradiation time. To demonstrate that the uptake of the AT101/LDL adduct by TUBO cells involves LDLRs, a competition assay with native LDL was carried out. After 16 hours of cell incubation in the presence of the AT101/LDL adduct (20 μg/mL), the uptake decreased by about 50% when the concentration of native LDL added to the culture medium was 200 μg/mL. Furthermore, in order to exclude that the AT101/LDL uptake is the consequence of a difference in the endocytosis rates of these cell lines, a comparison of non-targeted, Gd-DOTAMA(C18)$_2$ containing stealth liposomes[35] (LIPO) uptake has been carried out. Figure 2, *B* shows that the amount of internalized Gd is significantly lower than that measured upon AT101/LDL incubation in all considered tumor cells ($P < 0.0006$). On the contrary, the healthy N-MUG cells not showed a significant difference between LDL and LIPO ($P = 0.1$) indicating the not-specific endocytic uptake of both particles. In order to assess whether the amount of Gd internalized in target cells is enough to permit MRI visualization, T_1 weighted images of glass capillaries containing cellular pellets obtained by incubating TUBO cells with increasing amounts of LDL/AT101 were acquired at 7 T (Figure 2, *C*). The T_1 weighted image shows clearly that the SI of cells incubated in the presence of LDL/AT101 is hyperintense in comparison with the control. As expected the SI is directly proportional to the LDL concentration.

Evaluation of the AT101/LDL particle uptake "in vivo" in pulmonary metastasis

In order to generate the lung metastasis mice model, 50000 TUBO cells have been injected intravenously (iv) 3 weeks before MRI analysis and BNCT treatment. At this time all mice develop many pulmonary metastasis of 0.5-2 mm diameter. Tumor bearing mice ($n = 4$) received (iv) a bolus of AT101/LDL at a dose of 0.1 mmol kg^{-1} as expressed in terms of Gd content. T_1-weighted spin-echo MR-images were acquired before and 3, 6, and 24 hours after the CA administration. Representative examples of axial T_1-images of lung metastases acquired before and 3 hours after LDL/AT101 injection are reported in Figure 3, *A* and *B*, respectively. Figure 3, *C* reports the mean SI enhancement (%) at the different time intervals. As expected, high % SI enhancement are observed in the tumor region and in the liver due to the high LDLRs expression on both tumor cells and normal hepatocytes. On this basis, the liver has to be protected with a neutron shield during BNCT treatment.

The *boron* concentrations calculated at 3, 6 and 24 hours post-injection, using the method reported above, in the tumor, muscle (surrounding lungs), and liver are reported in Table 1. The intra-tumor *boron* concentration was significantly above the established threshold of 20/30 ppm, which is suitable for efficient BNCT treatment. The ratio of the concentration of *boron* atoms derives from the comparison between the concentrations in the tumor and surrounding muscle. On the basis of these results 6 hours POST i.v. has been selected as the best time to perform BNCT. In fact, at this time, the high *boron* concentration in tumor (48 ppm) is combined with a high tumor/muscle *boron* ratio that is fundamental to avoid healthy tissues damage.

BNCT treatment of TUBO cells "in vitro"

For the BNCT studies the AT101 ligand has been chelated to Gd^{3+} enriched in the isotope 157. Seven T75 flasks, four with TUBO cells previously incubated for 16 hours in the presence of AT101/LDL (50 μg/mL protein concentration), and three with non-treated control cells were irradiated in the thermal column of the TRIGA Mark II reactor for 15 minutes. *Boron* concentration inside TUBO cells during the irradiation was of 36 ppm. At the end of irradiation the medium was removed and replaced with fresh DMEM and flasks were placed at 37 °C in a humidified atmosphere of 5% CO_2. After 24 hours cells were detached, counted and re-plated to follow their proliferation. Two cell controls have been used in this experiment. The first did not receive any neutron irradiation and any *boron* containing compound and the second control was irradiated without the

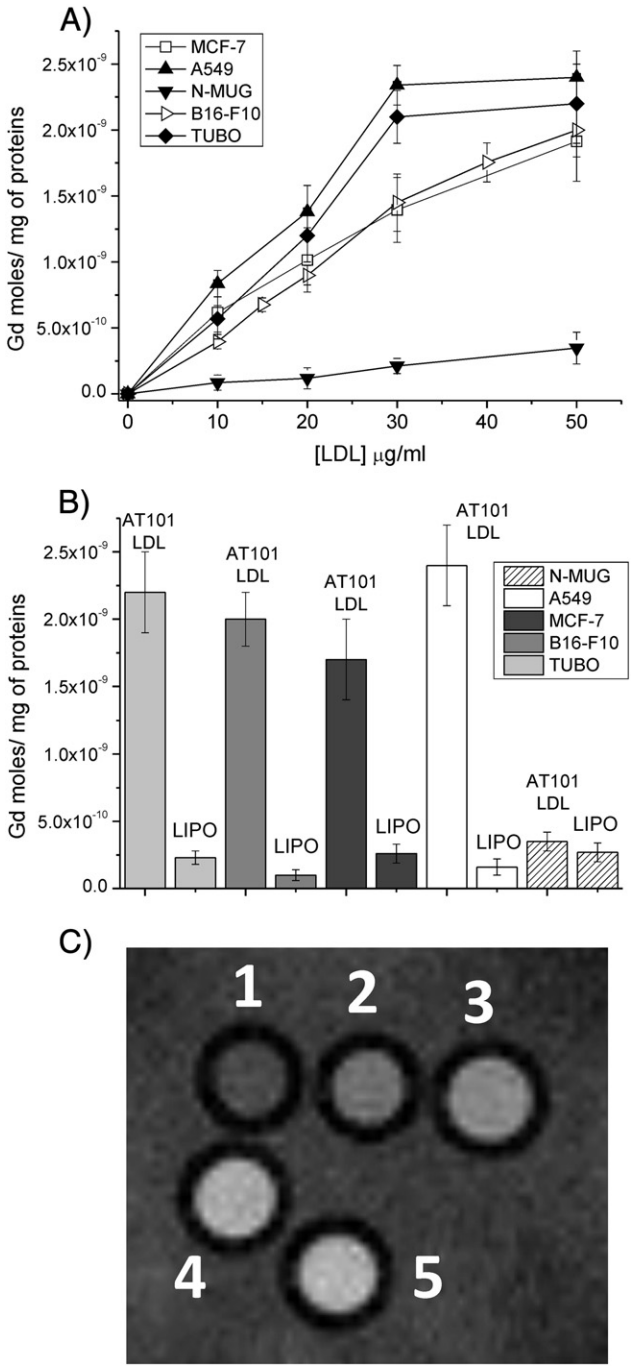

Figure 2. **(A)** "In vitro" uptake experiments onTUBO, B16-F10, MCF-7, A549 and N-MUG cell lines. Cells were incubated for 16 hours at 37 °C in the presence of increasing amounts of AT101/LDL (expressed as protein concentration μg/mL). The amount of Gd taken-up by cells has been determined by ICP-MS and it was normalized to the protein content determined by the Bradford assay. Errors bars report the standard deviation (SD) of the data. **(B)** Student two-tailed t test comparison of AT101/LDL and Gd-liposome (LIPO) cell uptake: TUBO ($P = 0.0002$); B16-F10 ($P = 0.00004$); MCF7 ($P = 0.0006$); A549 ($P = 0.0001$); N-MUG ($P = 0.1$). Cells were incubated for 16 hours at 37 °C in the presence of 20 μM Gd concentration in both LDL and LIPO conditions. A P value less than 0.05 was considered statistically significant. Data are expressed as means ± SD. **(C)** T_1-weighted spin-echo MR image of an agar phantom with glass capillaries containing unlabeled cells (1) and cells incubated with 10, 20, 30 and 50 μg/mL of AT101/LDL (2-5, respectively) for 16 hours at 37 °C.

administration of the *boron* containing compound. The proliferation rate of the *boron* treated cells survived to the irradiation is significantly lower than the rates measured for both control cells (Figure 4). On this basis one can conclude that the intracellular *boron* amount is sufficient to induce a dramatic toxic effect upon neutron flux exposure.

Irradiation set-up and radiation dose calculations

Mice neutron irradiation was carried out using the same irradiation facility used for cells. To limit the neutrons dose absorbed by the liver and spleen, as AT101/LDL accumulate in these organs and to limit the neutron-induced radioactivity in the whole animal, neutron-absorbing shields made of 95% ^{6}Li-enriched Li_2CO_3 powder have been used leaving only the thorax region, in correspondence of lungs, exposed to the neutron flux (Figure S2 supplementary materials). To know the radiation doses delivered in the tumor and in the healthy tissues/organs, a simulation program dedicated to neutron and photon transport in complex geometries (MCNP) was used. The radiation/material interaction is carefully reproduced thanks to point-wise nuclear cross data. Using B concentrations measured by MRI and MCNP simulation, the total dose (Dtot) absorbed by the tissues was calculated as well as the various dose components arising from: i) high linear energy transfer (LET) protons emitted by neutron capture reaction on ^{14}N and by elastic scattering on ^{1}H (% protons); ii) secondary radiations emitted by neutron capture reaction on ^{10}B (therapeutic fraction; % ^{10}B NCT); iii) γ-rays, including the photon contamination of the incident neutron beam (facility background) iv) 2.2 MeV γ-ray of thermal neutron capture reaction on ^{1}H (% γ-rays) (Tables 2 and 3).

To carry out a safe treatment, preliminary irradiations of wild type BALB/c mice ($n = 15$) were performed using the described shielding without the administration of the *boron* containing compound. The irradiation time was increased from 10 up to 20 minutes, while the reactor power was kept at 250 kW. From these results (reported as supplementary materials in Figure S3), the time for the NCT irradiation was fixed to 15 minutes, taking into account the toxicity just described and the presence, during a real NCT, of the enhancement capture agents in the tissues. To assess the safety of this treatment plan, the doses were compared to a tolerance limit of about 7 Gy delivered in a total body X- or γ-ray irradiation of the mouse.[36] The dose contribution due to the 92.3% enrichment in ^{157}Gd was calculated as well. As anticipate, the biological effect was mainly expected from the Auger electrons which transport a very little fraction of the total energy emitted by ^{157}Gd capture reaction. As consequence, the contribution of this radiation in term of absorbed dose is pretty low. The MCNP simulations reported an enhancement of the total doses showed in Table 2 of about 5-6% in the lung metastases, while the same increment can be as high as around 10% in healthy tissues, depending on Gd concentration and organ position and shielding.

BNCT treatment of pulmonary metastasis

BALB/c mice ($n = 40$) received an i.v. injection of 50000 TUBO cells 3 weeks before BNCT treatment. This led to the formation of several pulmonary metastases that have been visualized by MRI using a T_2-weighted RARE sequence. The

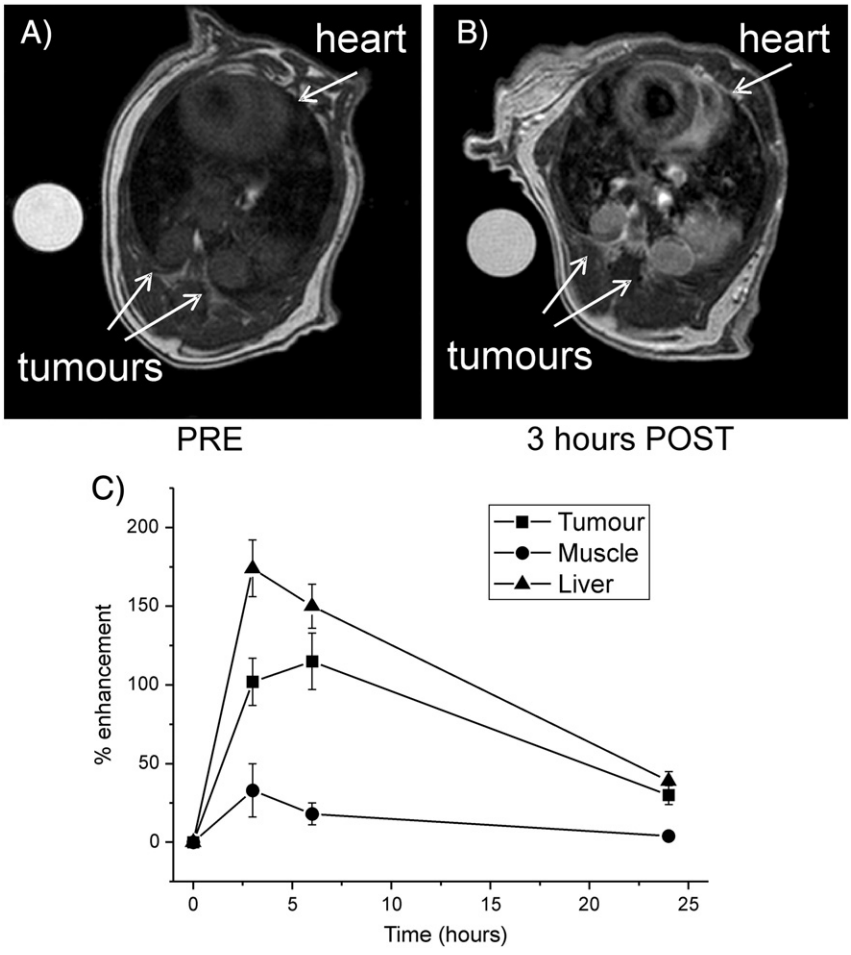

Figure 3. MRI "in vivo" in BALB/c mice with pulmonary metastases after administration of the AT101/LDL nanoparticles. Representative T_1-weighted MR images of BALB/c lungs acquired before **(A)** and 3 hours after **(B)** the administration of AT101/LDL particles. **(C)** A plot of MRI SI enhancements (%) measured in different organs vs. time after the administration of the AT101/LDL adduct. Error bars report the SD.

Table 1
Biodistribution of *boron* atoms in lung metastases bearing mice.

Time POST i.v.	Tumor B ppm	Muscle B ppm	Liver B ppm	Ratio of B atoms in tumor/muscle
3 hours	41 ± 9	15 ± 5	73 ± 18	2.7:1
6 hours	48 ± 11	9 ± 3	63 ± 12	5.3:1
24 hours	13 ± 5	2 ± 1	16 ± 6	6.5:1

number of metastasis varied markedly from mouse to mouse (from 5 to 20). The intratumor *boron* concentration has been determined by MRI 3 hours after the AT101/LDL administration and was of 43 ± 10 ppm whereas 16 ± 5 *boron* ppm have been found in the surrounding healthy muscle. Two groups of animals (n = 15 for each group) underwent the irradiation treatment. The first group received AT101/LDL at a Gd dose of 0.1 mmol/kg corresponding to a *boron* dose of 10 mg/kg, 6 hours before neutron exposure. The second group (irradiated control group) received the same volume of PBS to assess the effect of neutron irradiation in the absence of AT101/LDL. A third group of non-irradiated mice (n = 10) was used as a reference to assess tumor growth in the absence of any treatment and irradiation.

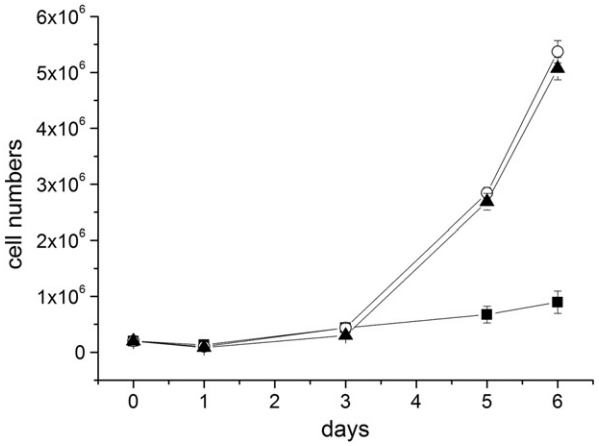

Figure 4. Proliferation curve of: not irradiated (○), irradiated (▲) TUBO control cells, and irradiated (■) TUBO cells after B treatment. Cells were re-plated 24 hours after the BNCT treatment.

Tumor size has been monitored by MRI using a T_2-weighted RARE sequence (Figure 5, *A-D*). No growth of the tumor size was detected for irradiated and treated animals in the first

Table 2
MCNP-simulated total absorbed dose (Dtot) and its components when animals are irradiated and treated with AT101/LDL adduct (mean neutron fluence of about $1.3 \cdot 10^{12}$ cm^{-2}).

Tissue/organ	B10 ppm	Dtot (Gy)	% protons	% B10 NCT	% γ-rays	% γ-rays from facility background
Lung metastases	43	5.6-7.3	4.7	70.8	24.5	23.6
Lung	16	3.6	9.6	46.4	44.0	42.1
Liver	43	4.9	6.0	61.2	32.8	30.8
Kidney	43	4.1-4.4	5.4	57.3	37.3	35.4
Small bowel	16	2.0	6.3	15.6	78.1	75.5
Brain	16	1.9	2.3	16.1	81.6	78.4
Whole body	16	2.7	8.4	33.6	58.0	55.9

Table 3
MCNP-simulated total absorbed dose (Dtot) and its components when the animal undergoes neutron irradiation only (mean neutron fluence of about $1.3 \cdot 10^{12}$ cm^{-2}).

Tissue/organ	Dtot (Gy)	% protons	% γ-rays	% γ-rays from facility background
Lung metastases	1.8-1.9	16.4	83.6	80.6
Lung	1.9	17.9	82.1	78.5
Liver	1.9	15.5	84.5	79.4
Kidney	1,8	12.6	87.4	82.9
Small bowel	1.7	7.4	92.6	89.4
Brain	1.6	2.8	97.2	93.5
Whole body	1.8	12.7	87.3	84.3

25 days after BNCT (Figure 5, *E*). Only at longer times the tumor lesions slowly restarted their growth.

BNCT treatment of EML4-ALK transgenic mice

EML4-ALK transgenic mice received the same treatment described above. At the day of irradiation, the tumor volumes of 6 weeks old EML4-ALK mice were between 0.5-15 mm^3 (Figure 6, *A*). *Boron* concentrations were calculated 3 hours before BCNT treatment by MRI measuring the SI enhancement in the tumor regions in the T_1 weighted images before and after the AT101/LDL administration and they were of 52 ± 12 and 16 ± 5 ppm in the tumor and surrounding muscle, respectively. On this basis it is possible to conclude that also in this model the intratumor amount of *boron* was enough to expect a significant regression of the tumor mass upon the neutron exposure. A limited toxic effect on the surrounding muscle is expected thanks to the three times lower *boron* concentration detected in these healthy tissues. Two groups of mice have been considered in this study. The first group (n = 5) received AT101/LDL in a Gd dose of 0.1 mmol/kg, 6 hours before neutron exposure. The second group (irradiated control group; n = 5) received the same volume of PBS in order to assess the effect of neutron irradiation in the absence of AT101/LDL. Figure 6, *B* shows that the tumor growth of mice irradiated after *boron* treatment was negligible for the first 30 days.

Discussion

The proposed procedure, based on the destruction of the tumor bulk by BNCT using a *boron*/Gd dual nanosized delivery agent, opens a promising therapeutic opportunity for lung cancer treatments in particular in the presence of disseminated tumors. This approach has been tested on mammary metastases (obtained by injecting i.v. mammary carcinoma TUBO cells) and ALK-EML4 transgenic mouse models of lung carcinogenesis, that develop highly aggressive tumors with modality similar to that of human cancer. In this contest, the possibility to measure *boron* concentration indirectly by MRI exploiting the presence of the conjugated Gd CA, was fundamental to proceed with the best treatment duration, at the most advantageous time after boron administration and with a proper neutron fluence. In fact, successful results can only be expected if a sufficient dose is delivered to tumor while the dose absorbed to normal tissues is kept under the tolerance dose. In order to achieve this result, a combination of three factors is necessary: a suitable boron concentration in the tumor, a high tumor to normal tissue ratio and a sufficient neutron flux to irradiate animals in acceptable times. The observed tumor re-growth observed on both mice models about 25-30 days after the treatment may be accounted in terms of two possible explanations: i) it might be associated to the presence in the tumor mass of quiescent cells, for which a greater capacity to recover from radiation and chemotherapeutic agent-induced damage has been demonstrated.[37,38] In addition, the higher resistance observed for these cells to targeted therapies could be the consequence of a lower expression of target receptors with respect to highly proliferating cells; ii) the neutron dose delivered to the lung tumor is not sufficient to kill all the cells. This may be due to the fact that the shielding set-up is a compromise between the need to protect the animal and the therapeutic effect gained by neutron irradiation. Actually, due to the proximity of lungs and liver, organs where AT101/LDL accumulates, it is difficult to design and locate the lithium carbonate shield in a way that the healthy tissue is preserved

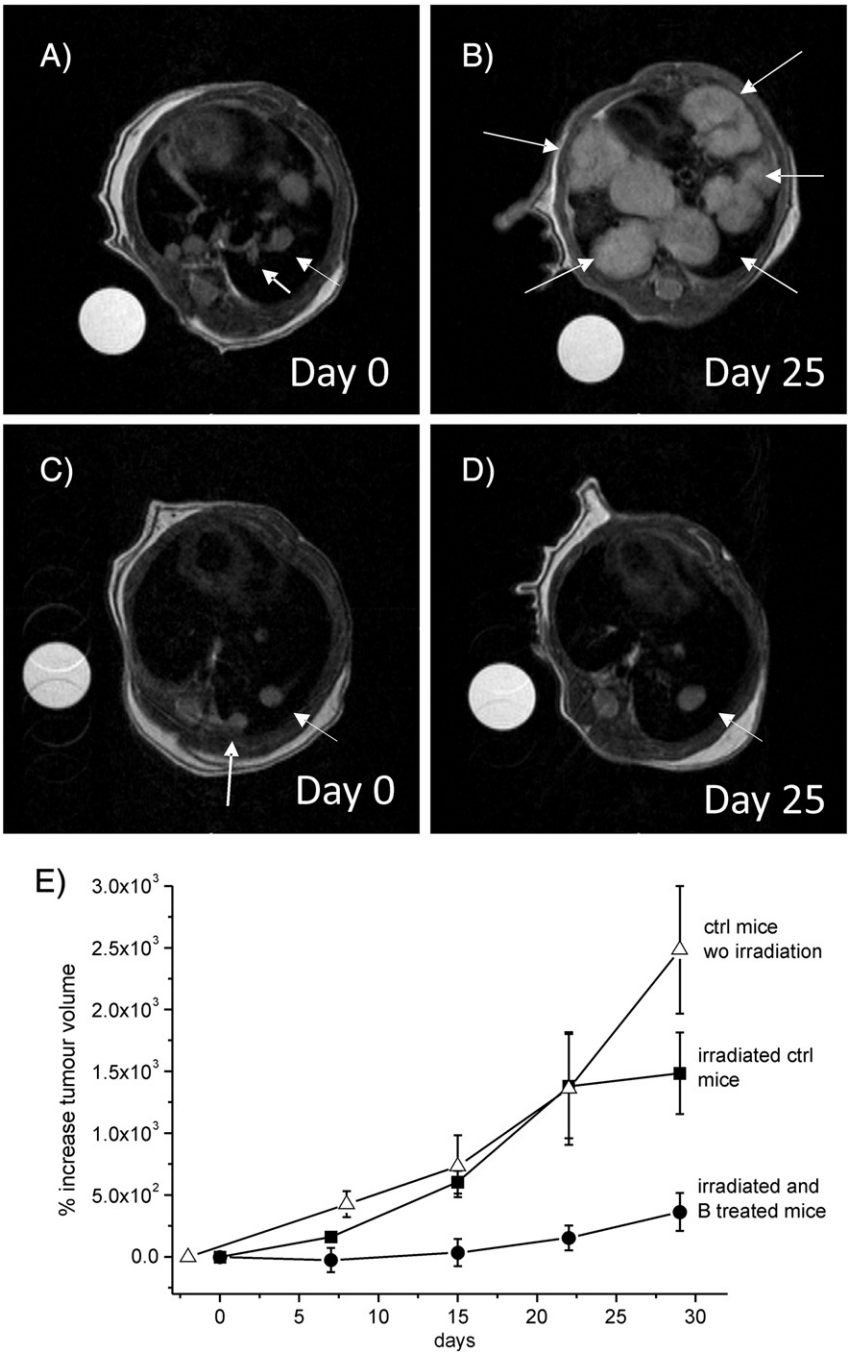

Figure 5. Tumour-growth evaluation performed after neutron irradiation. T_2-weighted RARE images acquired on lung metastases irradiated with neutrons without **(A,B)** or after **(C,D)** administration of AT101/LDL. (A) and (C) images were acquired at time 0 and (B) and (D) 25 days after neutron irradiation. In all images the arrows indicate tumour regions. **(E)** Tumour volumes increase measured by MRI on untreated control mice (Δ), irradiated control mice (■) and irradiated and AT101/LDL treated mice (●). Error bars indicate the SD.

while leaving the tumor exposed to neutron irradiation. This problem is essentially related to the small size of the animal and can be overcome in clinical applications where a collimated and selective neutron beam is used. Furthermore, as a consequence of the genetic origin of the ALK-EML4 mice model, one week after neutron irradiation, a formation of new tumor masses was observed. At the time of irradiation these small tumor masses were completely absent and therefore not affected by the neutron treatment, or their diameter was <0.2 mm and not detectable by MRI. The uptake of AT101/LDL administered intravascularly is reduced in the case of small lesions because they have not yet formed a distributed vascular system through which *boron* delivery takes place.

Finally, from these results one can surmise that it may be a worth to seek for the combination of BNCT with the administration of chemotherapic agents as well as with a different

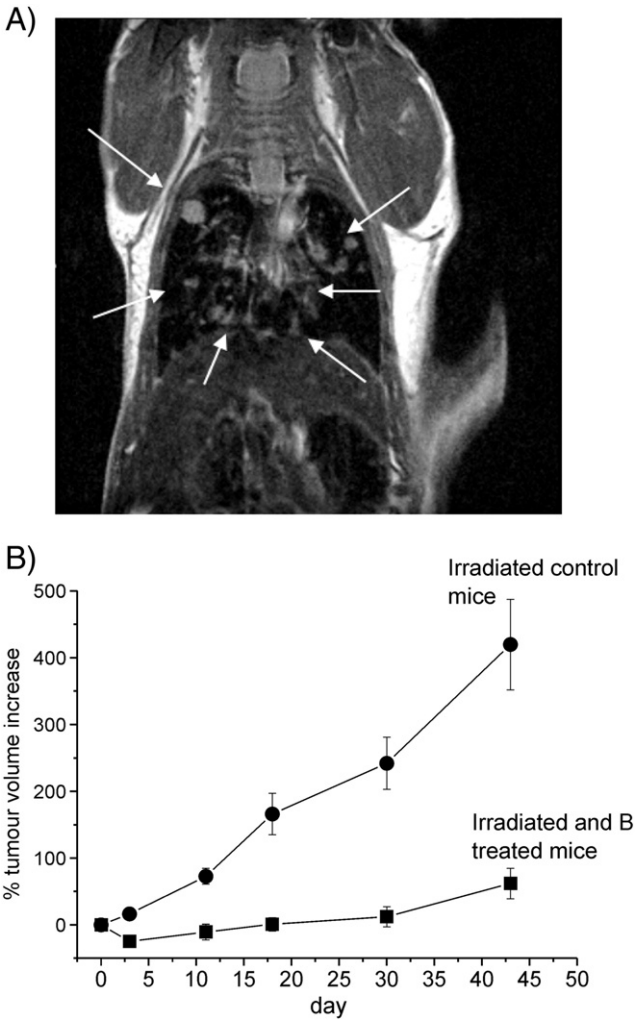

Figure 6. **(A)** T_2-weighted RARE coronal image of a representative 6 weeks old EML4-ALK mouse. Disseminated tumors are clearly visible in both lungs and they are indicated with arrows. **(B)** Tumor volumes increase measured by MRI on irradiated control mice (●) and irradiated and AT101/LDL treated mice (■). Error bars indicate the SD.

therapeutic strategy such us photodynamic therapy. These treatments should be administered 30-40 days after neutron irradiation when the bulk tumor mass is significantly reduced.

Supplementary data

Supplementary data to this article can be found online at http://dx.doi.org/10.1016/j.nano.2014.12.004.

References

1. Kankaanranta L, et al. Boron neutron capture therapy in the treatment of locally recurred head-and-neck cancer: final analysis of a phase I/II trial. *Int J Radiat Oncol Biol Phys* 2012;**82**:67-75.
2. Menéndez PR, Roth BM, Pereira MD, Casal MR, González SJ, Feld DB, Santa Cruz GA, Kessler J, Longhino J, Blaumann H, Jiménez Rebagliati R, Calzetta Larrieu OA, Fernández C, Nievas SI, Liberman SJ. BNCT
3. Andersen KF, Altaf R, Krarup-Hansen A, Kromann-Andersen B, Horn T, Christensen NJ, Hendel HW. Malignant pheochromocytomas and paragangliomas—the importance of a multidisciplinary approach. *Cancer Treat Rev* 2011;**37**:111-9.
4. Barth RF, Vicente MG, Harling OK, Kiger III WS, Riley KJ, Binns PJ, Wagner FM, Suzuki M, Aihara T, Kato I, Kawabata S. Current status of boron neutron capture therapy of high grade gliomas and recurrent head and neck cancer. *Radiat Oncol* 2012;**29**(7):146-7.
5. Barth RF. Boron neutron capture therapy at the crossroads: challenges and opportunities. *Appl Radiat Isot* 2009;**67**:S3-6.
6. Barth RF, Coderre JA, Vicente MG, Blue TE. Boron neutron capture therapy of cancer: current status and future prospects. *Clin Cancer Res* 2005;**1**(11):3987-4002.
7. Hawthorne MF, Lee MW. A critical assessment of boron target compounds for boron neutron capture therapy. *J Neurooncol* 2003;**62**:33-45.
8. Yamamoto T, Nakai K, Matsumura A. Boron neutron capture therapy for glioblastoma. *Cancer Lett* 2008;**262**:143-52.
9. Valliant JF, Guenther KJ, King AS, Morel P, Schaffer P, Sogbein OO, Stephenson KA. The medicinal chemistry of carboranes. *Coord Chem Rev* 2002;**232**:173-230.
10. Wu G, Barth RF, Yang W, Lee RJ, Tjarks W, Backer MV, Backer JM. Boron containing macromolecules and nanovehicles as delivery agents for neutron capture therapy. *Anticancer Agents Med Chem* 2006;**6**:167-84.
11. Crossley EL, Ziolkowski EJ, Coderre JA, Rendina LM. Boronated DNA-binding compounds as potential agents for boron neutron capture therapy. *Mini Rev Med Chem* 2007;**7**:303-13.
12. Bregadze VI, Sivaev IB, Glazun SA. Polyhedral boron compounds as potential diagnostic and therapeutic antitumor agents. *Anticancer Agents Med Chem* 2006;**6**:75-109.
13. Pak RH, Primus FJ, Rickard-Dickson KJ, Ng LL, Kane RR, Hawthorne MF. Preparation and properties of nido-carborane-specific monoclonal antibodies for potential use in boron neutron capture therapy for cancer. *Proc Natl Acad Sci U S A* 1995;**92**:6986-90.
14. Kueffer PJ, Maitz CA, Khan AA, Schuster SA, Shlyakhtina NI, Jalisatgi SS, Brockman JD, Nigg DW, Hawthorne MF. Boron neutron capture therapy demonstrated in mice bearing EMT6 tumors following selective delivery of boron by rationally designed liposomes. *Proc Natl Acad Sci U S A* 2013;**110**:6512-7.
15. Nakamura H. Boron lipid-based liposomal boron delivery system for neutron capture therapy: recent development and future perspective. *Future Med Chem* 2013;**5**:715-30.
16. Toppino A, Bova ME, Geninatti Crich S, Alberti D, Diana E, Barge A, Aime S, Venturello P, Deagostino A. A carborane-derivative "click" reaction under heterogeneous conditions for the synthesis of a promising lipophilic MRI/GdBNCT agent. *Chemistry* 2013;**19**:721-8.
17. Geninatti-Crich S, Alberti D, Szabo I, Deagostino A, Toppino A, Barge A, Ballarini F, Bortolussi S, Bruschi P, Protti N, Stella S, Altieri S, Venturello P, Aime S. MRI-guided neutron capture therapy by use of a dual gadolinium/boron agent targeted at tumour cells through upregulated low-density lipoprotein transporters. *Chemistry* 2011;**17**:8479-86.
18. Setiawan Y, Moore DE, Allen BJ. Selective uptake of boronated low-density lipoprotein in melanoma xenografts achieved by diet supplementation. *Br J Cancer* 1996;**74**:1705-8.
19. Savolainen S, et al. Boron neutron capture therapy (BNCT) in Finland: technological and physical prospects after 20 years of experiences. *Phys Med* 2013;**29**:233-48.
20. Geninatti-Crich S, Deagostino A, Toppino A, Alberti D, Venturello P, Aime S. Boronated compounds for imaging guided BNCT applications. *Anticancer Agents Med Chem* 2012;**12**:543-53.
21. Caravan P. Strategies for increasing the sensitivity of gadolinium based MRI contrast agents. *Chem Soc Rev* 2006;**35**:512-23.
22. Aime S, Cabella C, Colombatto S, Geninatti Crich S, Gianolio E, Maggioni F. Insights into the use of paramagnetic Gd(III) complexes in MR-molecular imaging investigations. *J Magn Reson Imaging* 2002;**16**:394-406.

23. Rovero S, Amici A, Di Carlo E, Bei R, Nanni P, Quaglino E, Porcedda P, Boggio K, Smorlesi A, Lollini PL, Landuzzi L, Colombo MP, Giovarelli M, Musiani P, Forni G. DNA vaccination against rat her-2/Neu p185 more effectively inhibits carcinogenesis than transplantable carcinomas in transgenic BALB/c mice. *J Immunol* 2000;**165**:5133-42.
24. O.A. Romero, S. Puertas, M. Vizoso, E. Nadal, T. Poggio, M. Sánchez-Céspedes, et al., Modeling lung cancer evolution and preclinical response by orthotopic mouse allografts.
25. Ng KK, Lovell JF, Zheng G. Lipoprotein-inspired nanoparticles for cancer theranostics. *Acc Chem Res* 2011;**44**(10):1105-13, http://dx.doi.org/10.1021/ar200017e [Epub 2011 May 10].
26. Firestone RA. Low-density lipoproteins as a vehicle for targeting antitumour compounds to cancer cells. *Bioconjug Chem* 1994;**5**:105-13.
27. Shih JL, Brugger RM. Gadolinium as a neutron capture therapy agent. *Med Phys* 1992;**19**:733-44.
28. Zonta A, et al. Extra-corporeal liver BNCT for the treatment of diffuse metastases: what was learned and what is still to be learned. *Appl Radiat Isot* 2009;**67**:S67-75.
29. Shiftan L, Israely T, Cohen M, Frydman V, Dafni H, Stern R, Neeman M. Magnetic resonance imaging visualization of hyaluronidase in ovarian carcinoma. *Cancer Res* 2005;**65**:10316-23.
30. Protti N, et al. *Gamma residual radioactivity measurements on rats and mice irradiated in the thermal column of a TRIGA Mark II reactor for BNCT purpose, accepted for publication by Health Physics Journal*; 2014.
31. Wetscott CH. Effective cross section values of well moderated thermal reactor spectra. *Rep AECL* 1960:1101-10.
32. Boggio K, Nicoletti G, Di Carlo E, Cavallo F, Landuzzi L, Melani C, Giovarelli M, Rossi I, Nanni P, De Giovanni C, Bouchard P, Wolf S, Modesti A, Musiani P, Lollini PL, Colombo MP, Forni G. Interleukin 12-mediated prevention of spontaneous mammary adenocarcinomas in two lines of Her-2/neu transgenic mice. *J Exp Med* 1998;**188**:589-96.
33. Li H, Gray BD, Corbin I, Lebherz C, Choi H, Lund-Katz S, Wilson JM, Glickson JD, Zhou R. MR and fluorescent imaging of low-density lipoprotein receptors. *Acad Radiol* 2004;**11**:1251-9.
34. Anelli PL, Lattuada L, Lorusso V, Schneider M, Tournier H, Uggeri F. Mixed micelles containing lipophilic gadolinium complexes as MRA contrast agents. *MAGMA* 2001;**12**:114-20.
35. Olson F, Hunt CA, Szoka FC, Vail WJ, Papahadjopoulos D. Preparation of liposomes of defined size distribution by extrusion through polycarbonate membranes. *Biochim Biophys Acta* 1979;**557**:9-23.
36. Upton AC, Conte FP, Hurst GS, Mills WA. The relative biological effectiveness of fast neutrons, x-rays, and gamma-rays for acute lethality in mice. *Radiat Res* 1956;**4**:117-31.
37. Masunaga SI, Sakurai Y, Tano K, Tanaka H, Suzuki M, Kondo N, Narabayashi M, Watanabe T, Nakagawa Y, Maruhashi A, Ono K. Effect of bevacizumab combined with boron neutron capture therapy on local tumor response and lung metastasis. *Exp Ther Med* 2014;**8**:291-301.
38. Masunaga S, Sakurai Y, Tanaka H, Suzuki M, Kondo N, Narabayashi M, Maruhashi A, Ono K. Wortmannin efficiently suppresses the recovery from radiation-induced damage in pimonidazole-unlabeled quiescent tumor cell population. *J Radiat Res* 2013;**54**:221-9.